iScience

Article

Optimal bandgap of a single-junction photovoltaic cell for the mobile Internet-of-Things

Graphical abstract

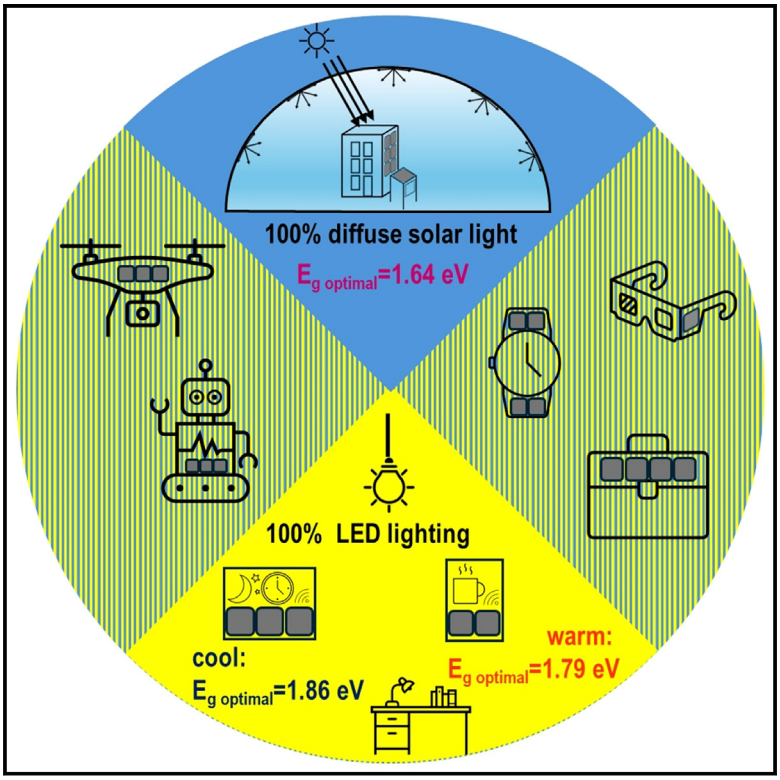

Highlights

- The procedure for determining the optimal gap for mobile photovoltaics is presented
- For large difference in irradiance, the analysis must be based on the power limit
- A gap of 1.64 eV is optimal for mobile IoT operating mainly outdoors

Authors

Grażyna Jarosz, Ryszard Signerski

Correspondence

grajaros@pg.edu.pl (G.J.),
ryssigne@pg.edu.pl (R.S.)

In brief

Energy engineering; Energy materials; Devices

Jarosz & Signerski, 2025, iScience *28*, 111604
January 17, 2025
https://doi.org/10.1016/j.isci.2024.111604

CellPress

iScience

CellPress
OPEN ACCESS

Article

Optimal bandgap of a single-junction photovoltaic cell for the mobile Internet-of-Things

Grażyna Jarosz[1,2,*] and Ryszard Signerski[1,*]
[1]Institute of Physics and Applied Computer Science, Faculty of Applied Physics and Mathematics, Gdansk University of Technology, ul. G. Narutowicza 11/12, 80-233 Gdańsk, Poland
[2]Lead contact
*Correspondence: grajaros@pg.edu.pl (G.J.), ryssigne@pg.edu.pl (R.S.)
https://doi.org/10.1016/j.isci.2024.111604

SUMMARY

The procedure for determining the maximum power of a single-junction photovoltaic cell operating in various types of lighting is presented. This is a key issue for photovoltaics powering the mobile Internet-of-Things (IoT). The simulations performed are based on the detailed balance principle, without any of the simplifying assumptions included in the Shockley-Queisser model. Optimal energy bandgap for diffuse solar light was found to be 1.64 eV with a cutoff generated power of 37.3 W/m^2. For the LED lighting considered in this work, the optimal energy bandgap and maximum power limit are 1.86 eV, 1.63 W/m^2, and 1.79 eV, 1.51 W/m^2 for cool and warm lighting, respectively, at 900 lux. Considering that the maximum power limit of diffuse solar radiation is much higher than the limit for LED lighting, we concluded that 1.64 eV is the optimal bandgap for most mobile IoT devices operating outdoors all or almost all the time.

INTRODUCTION

The development of the market for small Internet-of-Things (IoTs) devices, such as sensors, actuators, and wearables devices, creates a demand for a new type of photovoltaic cells (PV cells).[1–11] This means cells that could directly power small devices or charge their batteries and could operate effectively under the irradiation other than Standard Test Conditions.[12,13] The spectrum of the incident radiation, specifically its range and spectral width, determines the optimal energy bandgap and the efficiency limit of PV cells.[3–18] Therefore, the details of irradiation spectrum are essential to optimize the PV cell for a specific application. The starting point for obtaining the most efficient PV cell is the analysis of the thermodynamic curve of the efficiency limit as a function of the energy bandgap. This type of curve is well known for standard sunlight such as AM1.5G and AM1.5D[19] as well as for selected artificial light sources.[15,17,20–23] However, the limiting curve for diffuse sunlight has not been evaluated so far, and this issue is very important for mobile outdoor photovoltaic devices. Another omitted problem is the question about the optimal energy bandgap for the case when PV cell is intended for dynamic operation in two different irradiation environments.

PV cells for IoT can generally operate in a variety of lighting conditions. Schematic diagram of the cell operating conditions for IoT is presented in Figure 1. They can constantly work inside buildings,[9,21,24–28] thus constantly using artificial lighting. They can also work outdoors, but they do not have to face south and they can collect mainly diffuse solar radiation. You can also consider PV cells for small mobile devices, i.e., those that operate several hours a day in diffuse sunlight[29] and several hours a day in artificial light.[30,31] Such cells are the subject of this work.

The aim of this work is to analyze the efficiency limit of PV cells for mobile IoTs. Based on the simulation performed, the optimal energy gaps of single-junction cell and the limits of average power for two different lighting spectra were determined. The simulations carried out are based on the detailed balance principle, without any of the simplifying assumptions included in the Shockley-Queisser model. Indoor, outdoor, and mixed conditions of IoT environments are taken into account. The original procedure for determining the optimal energy bandgap for a mobile PV cell operating in two different lighting conditions is presented.

Theoretical Basis

The energy conversion efficiency limit is defined as the maximum efficiency of an ideal semiconductor cell at a given radiation. Such a cell is made of an ideal semiconductor, i.e., a semiconductor in which each absorbed photon generates an electron-hole pair, and at the same time the absorption only concerns photons with an energy greater than or equal to the bandgap of the semiconductor. On the other hand, a free electron can recombine with a hole to generate a photon, while non-radiative recombination does not occur in an ideal semiconductor. The current density per cell surface divided by the elementary charge (J/e) is written as the difference in the rate of generation of charge-carrier pairs caused by thermal as well as by additional radiation and the rate of radiative recombination resulting from luminescence:

$$\frac{J}{e} = G_T + G_I - R_L \qquad \text{(Equation 1)}$$

where G_T is the rate of generation of charge-carrier pairs by thermal radiation, G_I is the rate of generation of charge-carrier pairs

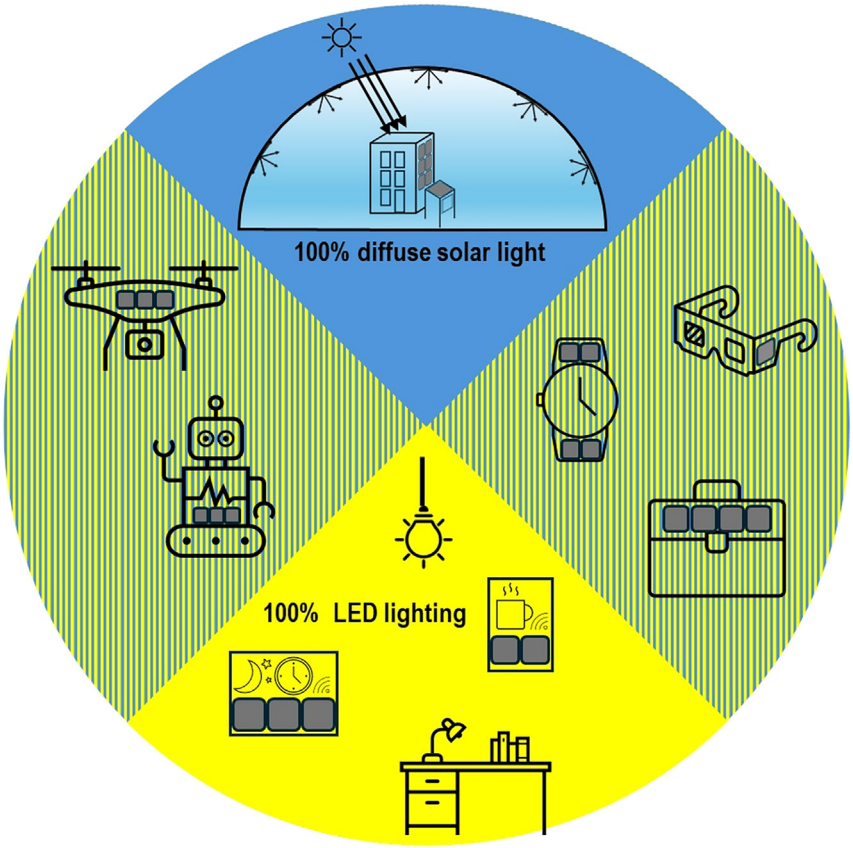

Figure 1. Schematic diagram of the cell operating conditions for IoT.

by illumination, and R_L is the rate of radiative recombination. All three rates are determined per unit of cell area.

The generation rates per unit cell surface can be written as:

$$G_T = \frac{1}{4\pi^2\hbar^3c^2}\int_{E_g}^{\infty}\frac{(E_{ph})^2}{\exp\left(\frac{E_{ph}}{kT}\right)-1}dE_{ph} \quad \text{(Equation 2)}$$

$$G_I = \int_{E_g}^{\infty}\frac{I(E_{ph})}{E_{ph}}dE_{ph} \quad \text{(Equation 3)}$$

where $\hbar$ is Planck's constant divided by 2π, c is speed of light in vacuum, E_g is energy bandgap of semiconductor, E_{ph} is photon energy, $I(E_{ph})$ is spectral irradiance expressed in W/(m^2eV), k is Boltzmann constant, T is absolute temperature of the cell, which, according to our assumption, is equal to ambient temperature.

If we assume that the back side of the cell is equipped with a mirror, effective recombination results only from the luminescence from the illuminated surface, which is expressed by the formula:

$$R_L = \frac{1}{4\pi^2\hbar^3c^2}\int_{E_g}^{\infty}\frac{(E_{ph})^2}{\exp\left(\frac{E_{ph}-\mu_C}{kT}\right)-1}dE_{ph} \quad \text{(Equation 4)}$$

where μ_C is chemical potential of the radiation emitted by the cell equal to the electrochemical potential of the cell, i.e., μ_C = eV where e is equal to the electron charge and V is equal to the voltage between the cell terminals.

Based on Equation 1 and using Equations 2–4 we can find current density-voltage characteristics (J-V) for any specific irradiation spectrum ($I(E_{ph})$) and any specific energy bandgap. The maximum electrical power delivered by a unit of cell area is the maximum product of J and V within the photovoltaic range. This point on the J-V curve is called the maximum power point (MPP), and its coordinates are known as V_{MPP} and J_{MPP}. The cell efficiency (η) for a specific $I(E_{ph})$ and a specific E_g gives the ratio of the maximum electrical power delivered by a unit cell surface to the radiation flux received by the unit cell surface, i.e., irradiation intensity,

$$\eta = \frac{J_{MPP}\cdot V_{MPP}}{\int_0^{\infty} I(E_{ph})dE_{ph}} \quad \text{(Equation 5)}$$

The relationships η vs. E_g can be derived from Equations 1–5 for a given $I(E_{ph})$ spectrum, after which $\eta(E_g)$ can be analyzed and the optimal E_g can be found. In the same way, the maximum power of a single-junction solar cell at a given $I(E_{ph})$ can be determined.

Illumination spectra

The offer of small devices included in the Internet-of-Thinks category is quite wide and is still growing. The devices are designed to work outdoor, indoor and at variable conditions. The latter are usually in constant motion with a person, animal or mobile system. They are then exposed partly to daylight and partly to artificial light.

In the case of mobile IoTs, you should not assume that these devices will track the position of the Sun in the sky. The assumption of free orientation of the PV cell is more justified. It can be assumed that such PV cells will process diffuse solar radiation. Therefore, the intensity of irradiance falling on a PV cell operating in such conditions can be expressed by the difference AM1.5G and AM1.5D:

$$I_{\lambda,DSR} = I_{\lambda,AM1.5G} - I_{\lambda,AM1.5D} \quad \text{(Equation 6)}$$

where $I_{\lambda,AM1.5G}$ is the spectral irradiance for AM1.5G, and $I_{\lambda,AM1.5D}$ is the spectral irradiance for AM1.5D. The AM1.5G denotes the hemispherical solar irradiance incident on a surface titled 37° toward the sun so consisting of both direct and diffuse

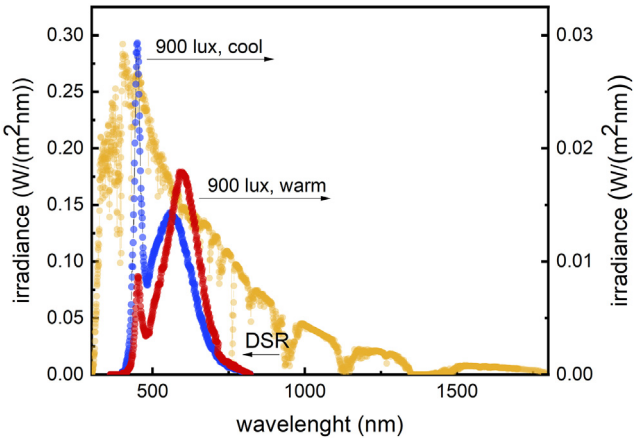

Figure 2. Irradiance spectra in the case of various lighting
DSR – diffuse solar radiation, 900 lux, cool – cool LED lighting, 900 lux, warm – warm LED lighting.

components. The AM1.5D is the direct irradiance including a circumsolar component for a field of view of 5.8° centered on the sun.[32] The integral of $I_{\lambda,DSR}$ overall wavelength values is 100.3 W/m^2.

Indoor lighting is currently provided by environmentally friendly light sources. These types of lamps do not emit any radiation beyond the visible range, so they do not convert electrical power into radiation invisible to the human eye. Since the luminous efficiency of any light source is defined as the ratio of the luminous flux to the electrical power, modern lamps are characterized by the highest luminous efficiency.[33]The spectrum of high-quality lighting should also cover the entire visible range reasonable well. The most economical solutions are white LEDs with luminophores and they currently dominate the lighting market. This type of lamps uses a blue LED, which excites the phosphor to luminance and is also a source of blue light. As a result, the spectrum of such a lamp consists of two peaks, a thinner one in the blue range emitted directly by the LED and much wider within green-red range coming from the phosphor. Of course, the intensity of illumination depends on the distance of the lamp from the object, the arrangement of lamps in space and the eye sensitivity curve. However, it can be assumed that the average illuminance of indoor objects with artificial light is 900 lux.[33]

Knowing the optical power spectrum ($P_{\lambda,optical}$ in W/nm), i.e., the spectrum of electromagnetic radiation emitted by lamp in the range from λ_i = 360 nm to λ_f = 830 nm, one can calculate the luminous flux (Φ_{lum} in lm) as follows[12,25,33]:

$$\Phi_{lum} = 683 \frac{lm}{W} \int_{\lambda_i}^{\lambda_f} V(\lambda)\, P_{\lambda,optical} d\lambda \qquad \text{(Equation 7)}$$

where V (λ) presents the tabulated values of the 2° degree CIE 1931 photopic eye sensitivity function,[34] λ_i and λ_f are the short-wave and long-wave limits of V(λ). Similarly, based on the irradiance spectrum (I_λ in W/(m^{2}nm)), we can determine the illuminance (I_{lx} in lx)[12,34,35]:

$$I_{lx} = 683 \frac{lm}{W} \int_{\lambda_i}^{\lambda_f} V(\lambda)\, I_\lambda d\lambda \qquad \text{(Equation 8)}$$

Figure 2 shows two typical irradiance spectra from white LED phosphor lamps for cool and warm lighting at illuminance equal to 900 lx. The presented spectra were obtained from real spectra multiplied by a certain coefficient selected so that I_{lx} determined on the basis of 8 was equal to 900 lx.

As can be seen, the spectral irradiance for white LED lamps is much narrower and one order of magnitude lower than for DSR. The total irradiance by white LED lamps is only 3.09 W/m^2 and 2.78 W/m^2 for the cool and warm lighting, respectively, shown in Figure 2. It is worth noting that the total irradiance is two orders of magnitude lower than in the case of DSR.

RESULTS AND DISCUSSION

Efficiency limit for diffuse solar radiation

Figure 3 shows the simulation results of the efficiency of ideal single-junction cell based on the procedure described in theoretical basis. The simulations used the spectrum of scattered sunlight obtained according to Equation 6 and presented in Figures 2 and 3 as a yellow series of dots. The efficiency curve reaches a maximum value of 37.23% for a cell with an energy bandgap of 1.64 eV. This value is almost 4% points higher than the efficiency of an ideal cell illuminated with AM1.5G [19]. The difference is directly related to the spectral widths of DSR and AM1.5G. However, due to the lower level of total irradiance, the power limit under DSR is almost an order of magnitude lower than with illumination by AM1.5G. Table 1 shows the values of the maximum efficiency and maximum power of a cell illuminated with DSR for selected values of semiconductor bandgap. The efficiency limit of an ideal cell exceeds 30% for a fairly wide bandgap range, i.e., from 1.09 eV to 2.27 eV, which allows for a fairly wide selection of semiconductor materials for cells intended to work with diffuse solar radiation.

Efficiency limit for white LEDs at 900 lux

The efficiency limits of a single-junction cell when exposed to white LED lighting at illuminance of 900 lx, at irradiance spectra shown in Figure 2, are shown in Figure 4. Additionally, Figure 4 presents the radiation spectra from Figure 2 as a function of photon energy. The maximum efficiency is 52.75% with a bandgap of 1.86 eV for cool illumination and 54.80% at a bandgap of 1.79 eV for warm illumination. The power limit achieved at these maximum values is 1.63 W/m^2 and 1.51 W/m^2 for warm and cool lighting, respectively. Due to the presence of an irradiation band only in the visible range, the efficiency limit shows a much higher and at the same time much narrower peak than in the case of DSR. Therefore, energy conversion efficiency values decrease rapidly as we move away from the optimal energy gap.

Table 2 shows the energy conversion efficiency limits and maximum power values of a single-junction cell for both types of artificial irradiance. The table shows the results for selected values of energy bandgap in the range from 1.00 eV

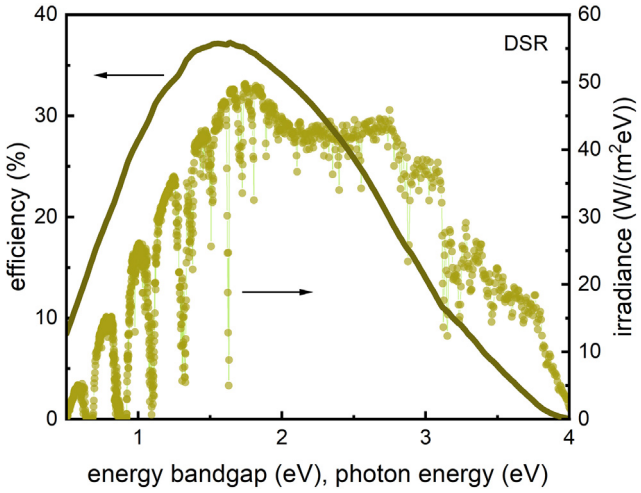

Figure 3. Efficiency limit of a single-junction cell as a function of the energy bandgap for diffuse sunlight radiation

Solid line – efficiency limit (Table S1), Series of dots – spectrum of diffuse solar radiation.

to 2.20 eV, also taking into account the optimal energy gaps for each lighting (shaded cells).

The optimal E_g for PV operating at different irradiations

As mentioned above, the maximum power of a PV cell and the optimal band gap of the cell depend on the irradiation spectrum. If the cell is designed to operate under two different lighting conditions, we can determine the energy conversion limit and the optimal band gap for each irradiation separately. If we can estimate the proportion between the cell exposure times in two different lighting conditions, then knowing the power limits as a function of bandgap, we can solve this problem in systematic way. Suppose the cell is exposed to DSR for a certain period of time during the day, say τ_2, and LED irradiation for a period of τ_1. The limit of the average power of such a cell in time $\tau_1+\tau_2$ can be determined as follows:

$$P_{av\ limit}(E_g) = \frac{\tau_1\, P_{max1}(E_g)+\tau_2\, P_{max2}(E_g)}{\tau_1+\tau_2} \qquad \text{(Equation 9)}$$

where $P_{max1}(E_g)$ and $P_{max2}(E_g)$ are power limits of a single-junction cell for the energy bandgap Eg under white LED and DSR, respectively. If $\tau_1+\tau_2$ is taken as 100% of the illumination time, then $\tau_1/(\tau_1+\tau_2)$ will be the part of the cell illumination time interval corresponding to illumination with artificial light. At the same time, $\tau_2/(\tau_1+\tau_2)$ will be the part of the lighting time corresponding to DSR. Let us denote the contribution of the cell irradiation by DSR as γ:

$$\gamma = \frac{\tau_2}{\tau_1+\tau_2} * 100\% \qquad \text{(Equation 10)}$$

Using definition (9), the limit of the average power of a single-junction cell ($P_{av\ limit}$) as a function of the energy bandgap for selected values of γ can be plotted. Figure 5 shows the $P_{av\ limit}$ as a function of the energy bandgap for four different lighting conditions: γ = 0% (cell exposed only to white LED), γ = 20%, γ = 40% and γ = 100% (cell exposed only to DSR). The peak of the $P_{av\ limit}(E_g)$ function determines the average power limit and the optimal energy bandgap of the cell operating in specific conditions, i.e., for a given γ. On this basis, it is possible to plot the relationship between the optimal energy gap of the cell and the average power limit of the cell as a function of γ. This relationship is shown in the insets of Figure 5.

From Figure 5 and Tables 1 and 2 it can be seen that the maximum power value of the cell illuminated by DSR is almost 25 times higher than the maximum power value of the cell illuminated with LED lamps. At the same time, you can notice a shift in optimal energy bandgap of the cell from 1.79 eV (for warm light) or from 1.86 eV (for cool light) to 1.64 eV. The optimal cell bandgap as a function of the parameter γ is shown in insets of Figure 5.

From Table 2, we conclude that the most desirable bandgap of PV cells for LED lighting is in the range of 1.79 eV–1.86 eV. The bandgaps of organic PV cells[36] as well as perovskite PV cells[37,38] are quite close to this range. Efficiency of 40% has already been reported for perovskite PV cells under artificial lighting.[39] On the other hand, the bandgaps of perovskite even better fit DSR than the white LED spectrum, so it can be expected that these materials will soon find application in mobile IoT.

Taking into account that the maximum power limit with DSR is much higher than the maximum power limit with white LED

Table 1. Efficiency and power limit of a single-junction cell under DSR

Energy bandgap (eV)	Efficiency (%)	Power limit (W/m²)	Energy bandgap (eV)	Efficiency (%)	Power limit (W/m²)	Energy bandgap (eV)	Efficiency (%)	Power limit (W/m²)
1.05	28.9	29.0	1.50	37.0	37.1	1.90	35.1	35.2
1.10	30.5	30.6	1.55	37.2	37.3	1.95	34.5	34.6
1.15	31.9	32.0	1.60	37.1	37.2	2.00	34.0	34.1
1.20	32.8	32.9	1.64	37.2	37.3	2.05	33.3	33.4
1.25	33.6	33.7	1.65	37.2	37.3	2.10	32.7	32.8
1.30	34.5	34.6	1.70	36.9	37.0	2.15	32.0	32.1
1.35	35.7	35.8	1.75	36.6	36.7	2.20	31.2	31.3
1.40	36.4	36.5	1.80	36.2	36.3	2.25	30.4	30.5
1.45	36.7	36.8	1.85	35.7	35.8	2.30	29.6	29.7

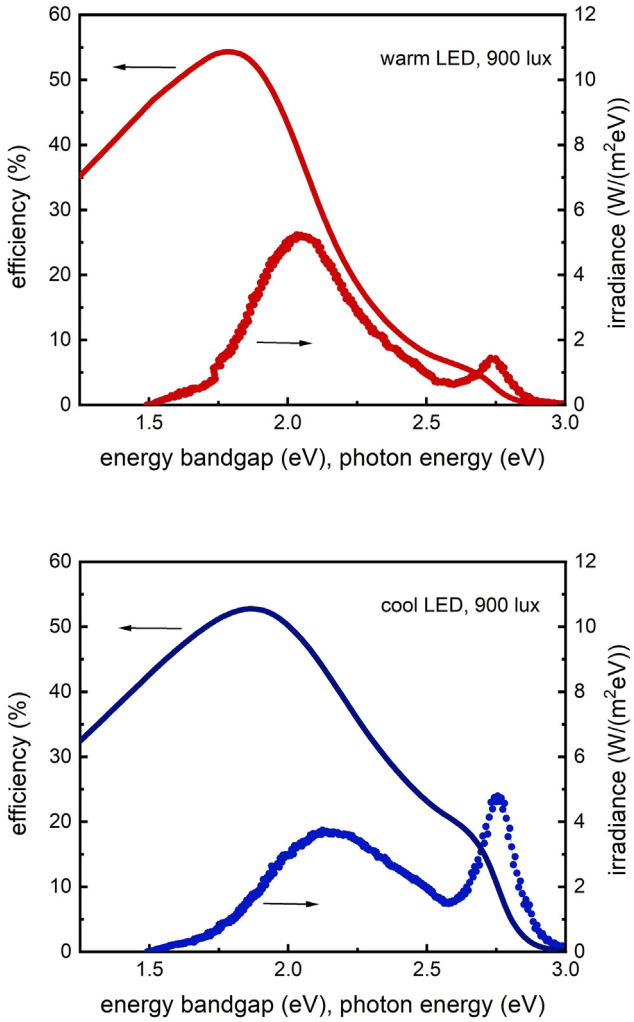

Figure 4. Efficiency limit of a single-junction solar cell as a function of the energy bandgap under artificial lighting

The irradiance spectra as a function of photons energy are shown as a series of dots and are the same as in Figure 2. Solid lines – efficiency limits (Table S2), Top graph – warm LED lighting, Bottom graph – cool LED lighting.

lamps, the optimal energy bandgap of the cell reaches a value of 1.64 eV already for $\gamma \cong 20\%$ (series of dots in the insets). The result of such a large difference is also a linear increase in the $P_{av\ limit}(E_g)$, which is observed for $\gamma > 20\%$ (solid line in the insets) and it results from the relationship:

$$P_{av\ limit}(E_g) = \frac{\gamma}{100\ \%} P_{max2}(E_{g\ optimal2}) \qquad \text{(Equation 11)}$$

met when

$$\gamma\ P_{max2}(E_{g\ optimal2}) \gg (100\ \%\text{-}\gamma)\ P_{max1}(E_{g\ optimal1}) \qquad \text{(Equation 12)}$$

where $P_{max2}(E_{g\ optimal2})$ is the maximum power limit for DSR, and $P_{max1}(E_{g\ optimal1})$ is the maximum power limit for white LED lighting.

Table 2. Limits of efficiency and power of a single-junction cell with white LED lighting

	warm light, 900 lx		cool light, 900 lx	
E_g (eV)	η (%)	P_{max} (W/m^2)	η (%)	P_{max} (W/m^2)
1.00	24.2	0.67	22.4	0.69
1.05	26.3	0.73	24.4	0.75
1.10	28.5	0.79	26.4	0.81
1.15	30.7	0.85	28.4	0.88
1.20	32.8	0.91	30.4	0.94
1.25	35.0	0.97	32.4	1.00
1.30	37.2	1.03	34.5	1.06
1.35	39.4	1.09	36.5	1.13
1.40	41.7	1.15	38.6	1.19
1.45	43.9	1.21	40.6	1.25
1.50	46.1	1.27	42.7	1.32
1.55	48.3	1.33	44.7	1.38
1.60	50.2	1.38	46.5	1.44
1.65	52.0	1.43	48.3	1.49
1.70	53.5	1.48	49.9	1.54
1.75	54.6	1.51	51.2	1.58
1.79	54.8	1.51	52.0	1.61
1.80	54.8	1.51	52.2	1.61
1.85	54.0	1.49	52.7	1.63
1.86	53.7	1.48	52.8	1.63
1.90	51.8	1.43	52.6	1.62
1.95	48.2	1.33	51.8	1.60
2.00	43.6	1.20	50.2	1.55
2.05	38.1	1.05	48.0	1.48
2.10	32.4	0.89	45.3	1.40
2.15	27.1	0.75	42.2	1.30
2.20	22.5	0.62	39.0	1.20

Finally, it is worth adding that determining the optimal cell energy bandgap for systems with different irradiation spectra requires analysis based on the cell power limit at different lighting conditions and cannot be based directly on the energy conversion efficiency. This is a direct result of the difference in irradiation power density. When this difference is significant, as in the above case, practically higher irradiation will determine the optimal energy gap and the limit of the average power of the cell.

Conclusions and limitations of the study

The work proposes a procedure for determining the optimal bandgap of a PV cell operating under two different types of lighting. This is a key aspect in the case of mobile photovoltaic systems. Such PV cells are used to power small Internet-of-Things systems. As shown, due to the usually large difference in total irradiation levels, the analysis in this case must be based on the power limit as a function of the energy bandgap rather than on the efficiency limit.

Based on the simulations performed, we found that the optimal energy gap of a single-junction cell for diffuse solar light

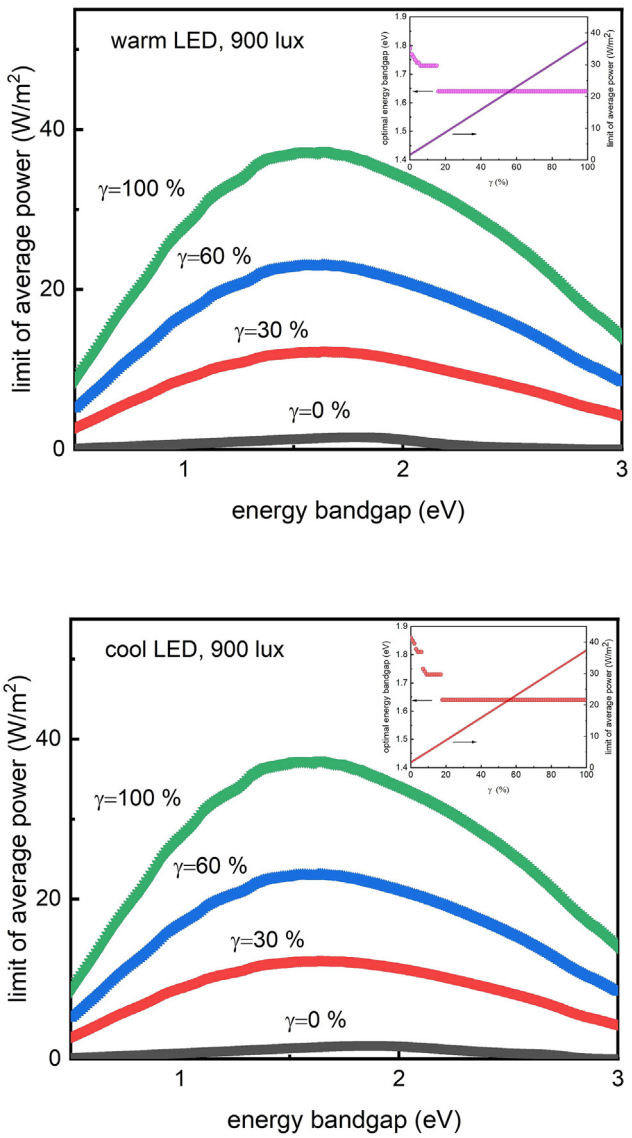

Figure 5. Average power limits as a function of the bandgap for different lighting conditions

Lighting conditions: γ = 0% (the cell exposed only to white LED lamp), γ = 20%, γ = 40%, γ = 100% (the cell exposed only to DSR), The insets show the optimal energy gap and average power limit as a function of γ (Table S3), Top graph – warm LED lighting, Bottom graph – cool LED lighting.

is 1.64 eV and the maximum power limit is 37.3 W/m^2. For LED lighting with the irradiance spectra shown in Figure 2, the optimal energy bandgap and maximum power limit of the cell are 1.86 eV, 1.63 W/m^2, and 1.79 eV, 1.51 W/m^2 for cool and warm lighting, respectively. Taking into account that the maximum power limit in the case of DSR is much higher than the limit in the case of white LED lighting, the optimal energy gap of the cell reaches a value of 1.64 eV already at 20% of the exposure time to DSR. We can therefore say that the bandgap of 1.64 eV is optimal for most mobile IoT devices operating outdoors all or almost all the time.

RESOURCE AVAILABILITY

Lead contact

Further information and requests should be directed to and will be fulfilled by the lead contact. Grażyna Jarosz (grajaros@pg.edu.pl).

Materials availability

This study did not generate new unique reagents.

Data and code availability

- Data: This paper is based on existing, publicly available data and on international standards. These accession numbers for the datasets are listed in the key resources table.
- Code: Widely known sources have been used and are mentioned in the key resources table. The original code is available on request from the lead contact.
- Other: Any additional information required to analyze the data or code reported in this paper is available from the lead contact upon request.

ACKNOWLEDGMENTS

This research was founded by the Institute of Physics and Applied Computer Science of Gdańsk University of Technology.

AUTHOR CONTRIBUTIONS

G.J. raised the issue. G.J. and R.S. designed simulations. G.J. performed simulations. G.J. and R.S. analyzed results and wrote the paper.

DECLARATION OF INTERESTS

The authors declare no competing financial interests.

STAR★METHODS

Detailed methods are provided in the online version of this paper and include the following:

- KEY RESOURCES TABLE
- EXPERIMENTAL MODEL AND STUDY PARTICIPANT DETAILS
- METHOD DETAILS
- QUALIFICATION AND STATISTICAL ANALYSIS

SUPPLEMENTAL INFORMATION

Supplemental information can be found online at https://doi.org/10.1016/j.isci.2024.111604.

Received: August 6, 2024
Revised: November 7, 2024
Accepted: December 11, 2024
Published: December 15, 2024

REFERENCES

1. Hamadani, B., Long, Y.-S., Tsai, M.A., and Wu, T.-C. (2021). Interlaboratory Comparison of Solar Cell Measurements Under Low Indoor Lighting Conditions. IEEE J. Photovoltaics *11*, 1430–1435. https://doi.org/10.1109/JPHOTOV.2021.3104144.
2. Chang, M.-C., and Liu, S.-I. (2020). An Indoor Photovoltaic Energy Harvester Using Time-Based MPPT and On-Chip Photovoltaic Cell. IEEE Trans. Circuits Syst. II. *67*, 2432–2436. https://doi.org/10.1109/TCSII.2020.2976760.
3. Jarosz, G., Marczyński, R., and Signerski, R. (2020). Effect of band gap on power conversion efficiency of single-junction semiconductor photovoltaic cells under white light phosphor-based LED illumination. Mater. Sci.

Semicond. Process. *107*, 104812. https://doi.org/10.1016/j.mssp.2019.104812.

4. Chmielewski, A., Szulim, P., Gregorczyk, M., Guminski, R., Mydłowski, T., and Mączak, J. (2017). Model of an electric vehicle powered by a PV cell – a case study. In 22nd International Conference on Methods and Models in Automation and Robotics (MMAR) (IEEE), pp. 1009–1014. https://doi.org/10.1109/MMAR.2017.8046968.
5. Ishiyama, T. (2022). Indoor Photovoltaic Energy Harvesting and Power Management for IoT Devices. In 11th IEEE Inter. Conf. on Renewable Energy Research and Applications, pp. 461–464.
6. Saad, P.,S.,M., Babri, M.,A.,H.,B., Hashim, H., and Shariffudin, S.,S. (2023). Dynamic Effect of Illumination on Single-Diode Photovoltaic Models: Performance Differences Between Indoor and Outdoor Environments. In IEEE International Conference on applied Electronics and Engineering (ICAEE 2023), pp. 1–5.
7. Manjhi, S., Siddharth, G., Pandey, S.,K., Sengar, B.S., Dwivedi, P., and Garg, V. (2023). Unveiling the Potential of Oxy-Iodide (BiOI)-Based Photovoltaic Device for Indoor Light Harvesting. IEEE Trans. Electron. Dev. *70*, 5690–5695. https://doi.org/10.1109/TED.2023.3308919.
8. Prabaswara, A., Browne, J., Zou, Y., King, R., Goodnick, S., and Corbett, B. (2022). Wide Band AlGaInP-based Photovoltaic Cell for Indoor Ambient Energy Harvesting. In IEEE 49th Photovoltaics Specialists- Conference, pp. 1159–1161.
9. Olzhabay, Y., Aidarkhanov, D., Ukaegbu, I.,A., and Ng, A. (2021). Performance Evaluation on Low Energy Consumption Devices Powered by Indoor Perovskite Solar Cells. In IEEE 48th Photovoltaic Specialists Conference (PVSC), pp. 1331–1335.
10. Müller, D., Jiang, E., Rivas-Lazaro, P., Baretzky, C., Loukeris, G., Bogati, S., Paetel, S., Irvine, S.,J.,C., Oklobia, O., Jones, S., et al. (2023). Indoor Photovoltaics for the Internet of Things – A Comparison of State-of-the-Art Devices from Different Photovoltaic Technologies. ACS Appl. Energy Mater. *6*, 10404–10414. https://doi.org/10.1021/acsaem.3c01274.
11. Hwang, S., and Yasuda, T. (2022). Indoor photovoltaic energy harvesting based on semiconducting π-conjugated polymers and oligomeric materials toward future IoT applications. Polym. J. *55*, 297–316. https://doi.org/10.1038/s41428-022-00727-8.
12. Michael, P.R., Johnston, D.,E., and Moreno, W.,A. (2023). Calculation of Irradiance from Illuminance for Artificial Light Photovoltaics Applications. IEEE Instrum. Meas. Mag. *26*, 52–58. https://doi.org/10.1109/MIM.2023.10121384.
13. Lynn, K. (2001). Test method for photovoltaic module rating. Florida Solar Energy Center (Publication FSEC-GP-68).
14. Würfel, P., and Würfel, U. (2016). Physics of Solar Cells (Weinheim: WILEY-VCH Verlag GmbH & Co. KGaA).
15. Jarosz, G., Franz, M., Marczyński, R., and Signerski, R. (2021). Efficiency limit of excitonic photovoltaic cells under phosphor-based white LED illumination. Org. Electron. *88*, 105999. https://doi.org/10.1016/j.orgel.2020.105999.
16. Zheng, C., Wu, Q., Guo, S., Huang, W., Xiao, Q., and Xiao, W. (2021). The correlation between limiting efficiency of indoor photovoltaics and spectral characteristics of multi-color white LED sources. J. Phys. D Appl. Phys. *54*, 315503. https://doi.org/10.1088/1361-6463/abfdda.
17. Saha, A., Haque, K.,A., and Baten, M.Z. (2020). Performance Evaluation of Single-Junction Indoor Photovoltaic Devices for Diufferent Absorber Bandgaps Under Spectrally Varying White Light-Emitting Diodes. IEEE J. Photovoltaics *10*, 539–545. https://doi.org/10.1109/JPHOTOV.2019.2959938.
18. Kumar, G., and Chen, F.-C. (2023). A review on recent progress in organic photovoltaic devices for indoor applications. J. Phys. D Appl. Phys. *56*, 353001. https://doi.org/10.1088/1361-6463/acd2e5.
19. Rühle, S. (2016). Tabulated values of the Shockley-Queisser limit for single junction solar cells. Sol. Energy *130*, 139–147. https://doi.org/10.1016/j.solener.2016.02.015.
20. Freunek, M., Freunek, M., and Reindl, L.,M. (2013). Maximum Efficiencies of Indoor Photovoltaic Devices. IEEE J. Photovoltaics *3*, 59–64. https://doi.org/10.1109/JPHOTOV.2012.2225023.
21. Kim, S.,H., Saeed, M.,A., Lee, S.,Y., and Shim, J.,W. (2021). Investigating the Indoor Performance of Planar Heterojunction Based Organic Photovoltaics. IEEE J. Photovoltaics *11*, 997–1003. https://doi.org/10.1109/JPHOTOV.2021.3074077.
22. Srivishnu, K.,S., Rajesh, M.,N., Prasanthkumar, S., and Giribabu, L. (2023). Photovoltaics for indoor applications: Progress, challenges and perspective. Sol. Energy *264*, 112957. https://doi.org/10.1016/j.solener.2023.112057.
23. Hou, X., Wang, Y., Lee, H.,K.,H., Datt, R., Uslar Miano, N., Yan, D., Li, M., Zhu, F., Hou, B., Tsoi, W.,C., and Li, Z. (2020). Indoor application of emerging photovoltaics – progress, challenges and perespectives. J. Mater. Chem. A *8*, 21503–21525. https://doi.org/10.1039/D0TA06950G.
24. Polyzoidis, C., Rogdakis, K., and Kymakis, E. (2021). Indoor Perovskite Photovoltaics for the Internet of Things – Challenges and Opportunities toward Market Uptake. Adv. Energy Mater. *11*, 2101854. https://doi.org/10.1002/aenm.202101854.
25. Li, B., Hou, B., and Amaratunga, G.A.J. (2021). Indoor photovoltaics, The Next Big Trend in solution-processed solar cells. InfoMat *3*, 445–459. https://doi.org/10.1002/inf2.12180.
26. Li, M., Igbari, F., Wang, Z.-K., and Liao, L.-S. (2020). Indoor Thin Film Photovoltaics: Progress and Challenges. Adv. Energy Mater. *10*, 2000641. https://doi.org/10.1002/aenm.202000641.
27. Ryu, H.,S., Park, S.,Y., Lee, T.,H., Kim, J.,Y., and Woo, H.,Y. (2020). Recent progress in indoor organic photovoltaics. Nanoscale *12*, 5792–5804. https://doi.org/10.1039/D0NR00816H.
28. Sampaio, P.,G.,V., and González, M.,O.,A. (2022). A review on organic photovoltaic cell. Int. J. Energy Res. *46*, 17813–17828. https://doi.org/10.1002/er.8456.
29. Macias, J., Herrero, R., José, L.,J.,S., Núñez, R., and Antón, I. (2024). On the optimization of the interconnection of photovoltaic modules integrated in vehicles. iScience *27*, 110089. https://doi.org/10.1016/j.isci.2024.110089.
30. Shakoor, W., and Khan, F. (2021). Solar Based Human Embedded Energy Harvester. In IEEE 2021 International Bhurban Conference on Applied Sciences and Technology, pp. 432–438.
31. Wu, D., Cui, Z., Xue, T., Zhang, R., Su, M., Hu, X., and Sun, G. (2023). Self-encapsulated wearable perovskite photovoltaics via lami-nation process and its biomedical application. iScience *26*, 107248. https://doi.org/10.1016/j.isci.2023.107248.
32. (2003). Standard Tables for Reference Solar Spectra Irradiances: Direct Normal and Hemispherical on 37° Tilted Surface (ASTM International).
33. Schubert, E.,F. (2006). Light-Emitting Diodes (New York: Cambridge University Press).
34. CIE 2018 (1931). CIE 1931 colour-matching functions , 2 degree observer (data table) (Vienna, Austria: International Commission on Illumination (CIE)). Technical report. https://cie.co.at/datatable/cie-1931-colour-matching-functions-2-degree-observer.
35. Hamadani, B.,H., and Campanelli, M.,B. (2020). Photovoltaic Characterization Under Artificial Low Irradiance Conditions Using Reference Solar Cells. IEEE J. Photovoltaics *10*, 1119–1125. https://doi.org/10.1109/JPHOTOV.2020.2996241.
36. Ko, S.,Y., Singh, R., Nketia-Yawson, B., Ahn, H., Jo, J.W., Lee, J.J., and Ko, M.J. (2021). Modulation of energy levels and vertical charge transport in polythiphene through copolymerization of non-fluorinated and fluorinated for organic indoor photovoltaics. Dyes Pigments *190*, 109292. https://doi.org/10.1016/j.dyepig.2021.109292.

37. Sujith, M., Prabu, R.,T., Kumar, A.K., and Kumar, A. (2024). Performance analysis of CsPbI3-based solar cells under light emitting diode illumination as an energy harvester for IoT and indoor photovoltaics. J. Comput. Electron. *23*, 866–873. https://doi.org/10.1007/s10825-024-02180-7.

38. Vanitha, L., Sahoo, S., Prabu, R.,T., and Kumar, A. (2024). Performance analysis of wide bandgap inorganic perovskite for indoor photovoltaics for IoT applications: simulation study. Opt. Quant. Electron. *56*, 1413. https://doi.org/10.1007/s11082-024-07336-0.

39. Singh, R., Nazim, M., Kini, G.,P., and Kan, Z. (2022). Perovskite-Based Photovoltaics for Artificial Indoor Light Harvesting: A Critical Review. Sol. RRL *7*, 2200953. https://doi.org/10.1002/solr.202200953.

STAR★METHODS

KEY RESOURCES TABLE

REAGENT or RESOURCE	SOURCE	IDENTIFIER
Software and algorithms		
Excel	Microsoft Excel	https://www.microsoft.com/pl-pl/microsoft-365/excel
Macros in Excel environment	Microsoft Excel	https://www.microsoft.com/pl-pl/microsoft-365/excel
Own algorithms on Macro procedures in Excel environment		
Other		
Spectra of AM1.G and AM1.5D	Standard Tables for Reference Solar Spectra Irradiances: Direct Normal and Hemispherical on 37° Tilted Surface, ASTM International G173-03 (Reapproved 2012).	https://standards.globalspec.com/std/14625520/astm-g173-23 https://standards.globalspec.com/std/14625520/astm-d173-23
Photopic eye sensitivity function	CIE 1931 colour-matching functions, 2° observer (data table), International Commission on Illumination (CIE)	https://cie.co.at/datatable/cie-1931-colour-matching-functions-2-degree-observer

EXPERIMENTAL MODEL AND STUDY PARTICIPANT DETAILS

This study did not need any experimental model.

METHOD DETAILS

The paper presents the results of simulations of the efficiency limit of photovoltaic cells under different lighting spectra. The simulations are based on the fundamental expressions of electron-hole pair generation and recombination in an ideal semiconductor, presented in theoretical basis. The numerical method uses multiple loops in Macros procedures so that none of the fundamental expressions are simplified or omitted. The numerical resolution for photons and voltage was as follows: δE_{ph} = 0.001 eV, δV = 0.001 V.

QUALIFICATION AND STATISTICAL ANALYSIS

The study does not include statistical analysis or quantification.